

Full moment tensor inversion for the 2013 Sea of Okhotsk deep earthquake

HARA, Tatsuhiko^{1*} ; KAWAKATSU, Hitoshi²

¹IISEE, BRI, ²Earthquake Research Institute, The University of Tokyo

We performed full moment tensor inversion for the May 24, 2013 Sea of Okhotsk deep earthquake, which is the largest deep earthquake (the moment magnitude is 8.3 after the Global CMT solution). Following Kawakatsu (1991), we redefined the diagonal components of the moment tensor, and determined full six component moment tensors. In order to determine the isotropic component independently from the CLVD component, we analyzed long period signals in the period range between 550 and 1000 s following Kawakatsu (1996), and Hara et al. (1995, 1996). We retrieved VHZ channel broadband waveform data from the IRIS DMC. The duration of the time series is five hours. We used the Direct Solution Method (Hara et al., 1991, 1993) to calculate the Green's functions. We considered the 3-D velocity structures of model SAW24B16 (Mégnin and Romanowicz, 2000) and crust 2.0 (Bassin et al., 2000; <http://igppweb.ucsd.edu/~gabi/rem.html>) to calculate synthetic seismograms. We set spatial grids around the PDE hypocenter for possible centroid locations and temporal grids around the centroid time of the Global CMT solution for possible centroid times. We conducted linear moment tensor inversions for pairs of the spatial and temporal grids to investigate the dependence of solutions on centroid location and time. In the preliminary analysis, the isotropic components of the solutions with larger variance reductions and smaller correlation coefficients with the isotropic component and the other moment tensor components are in the range around 2 to 4 per cent (implosive) of the seismic moment of this event. This preliminary result is consistent with Okal (2013), who obtained the implosive isotropic component with about 2 per cent of the seismic moment by the analysis of the normal modes ${}_0S_0$ and ${}_1S_0$, although further evaluation on uncertainty of the estimates obtained in this study is required.

Keywords: deep earthquake, moment tensor, isotropic component

Estimation of Radiated Seismic Energy from Teleseismic Body Waves

KIUCHI, Ryota^{1*} ; MORI, James¹

¹Disaster Prevention Research Institute, Kyoto University

Radiated seismic energy is a fundamental parameter for understanding source physics. Using teleseismic P waves, Choy and McGarr (2002) reported that strike-slip earthquakes in the oceanic lithosphere have high apparent stress (rigidity multiplied by the ratio of radiated energy to seismic moment). However, that estimates may have a large variation, because of the large radiation pattern of nodal arrivals. Therefore, we improved that used method to better correct for radiation pattern. From our result, we find that the strike-slip earthquakes have apparent stress values that are 5 to 8 times higher than dip-slip earthquakes with the oceanic events having slightly higher values than continental events. In addition, using our improved methods, we can estimate the apparent stresses for strike-slip earthquakes with more reliability, since the error of radiated seismic energies becomes smaller.

Keywords: Radiated seismic energy, Apparent stress, Strike-slip earthquake

Seismic energy estimation of repeating earthquake sequences offshore northeastern Japan

ARA, Masamichi^{1*} ; IDE, Satoshi¹ ; UCHIDA, Naoki²

¹The University of Tokyo, EPS, ²Graduate school of science Tohoku university

Repeating earthquakes are thought to occur on locked patches, which represent almost time-independent irregularity on the plate interface, to catch up with stable slip on the surrounding interface. Thus, they produce spatial and temporal stress heterogeneity around the source area, which may control the spatial and temporal patterns of seismic energy of repeating earthquakes. We estimate seismic energy for many small to moderate repeating earthquakes that occurred offshore northeastern Japan, to understand the nature of stress heterogeneity and hidden structural irregularity.

Seismic energy reflects dynamic fault motion during an earthquake, while seismic moment is determined by the difference between the initial and final states of the fault. Seismic moment is determined relatively precisely using the low frequency limit of seismic spectra. In contrast, seismic energy has large errors because it is determined from the entire frequency range of seismic spectra, after correcting path and site effects which can be significant especially at high frequencies. Another problem is the size dependence of seismic energy, which has been a matter of debate for two decades in seismological community. A typical question is whether scaled energy (the ratio of seismic energy to moment) is dependent on seismic moment. These problems have to be alleviated to discuss the spatial and temporal variation of radiated seismic energy. Seismic energy must be estimated as precise as possible.

As mentioned, the most serious problem in estimating seismic energy is removing path and site effects. To avoid this problem, the present study adopts an empirical Green's function (EGF) method. We regard the ratio of seismic spectra as the ratio of source spectra, since the seismic spectra of co-located events observed at one station share the same path and site effects. We modify an EGF method with coda waves developed by Baltay et al. (2010), to rigorously evaluate the uncertainty in corner frequencies and the effects of noise.

This method is applied to several repeating earthquakes of magnitude ~2 to 6 that occurred offshore northeastern Japan. We estimate seismic energy for a group of events by calculating the ratios of source spectra using S-coda waves in two horizontal components of Hi-net, National Research Institute for Earth Science and Disaster Prevention. The scaled energy is almost constant or slightly increasing with seismic moment. Nevertheless, the results are still tentative because the estimation of seismic energy is dependent on the assumption of source spectral model, such as the omega-square model, which have not been constrained well.

Stress drop variations among small earthquakes in the Tohoku-oki region - implications for the 2011 megathrust event

UCHIDE, Takahiko^{1*} ; SHEARER, Peter² ; IMANISHI, Kazutoshi¹

¹Geological Survey of Japan, AIST, ²Scripps Institution of Oceanography, UC San Diego

It is important to assess the likely rupture characteristics of future megathrust earthquakes. One approach is to study the spatio-temporal variation of geophysical properties in active subduction zones. We explore this idea by examining stress drops of 1536 small earthquakes (Mw 3.0 - 4.5) shallower than 80 km in the Tohoku-oki region before the 2011 Tohoku-oki earthquake. We estimate stress drops using the spectral analysis method described by Shearer et al. [2006], which isolates source, path, and receiver terms and then applies an empirical Green's function (EGF) correction before computing corner frequencies and stress drops using the Madariaga [1976] model.

We find an overall increase in stress drop with depth, as well as lateral variations in stress drop along strike. Higher-than-average stress drops are found in East Aomori-oki and Miyagi-oki, whereas Sanriku-oki is a moderate stress-drop area. The high stress-drop zone in Miyagi-oki is located just south of the large slip area of the 2011 Tohoku-oki earthquake, and possibly acted as a barrier to further rupture propagation during the event. The Miyagi-oki high-stress-drop zone is located on west of the 1978 Miyagi-oki earthquake rupture area.

Stress drops of earthquakes in the large slip patch of the 2011 Tohoku-oki earthquake are comparable to the mainshock stress drop. Since studies [Hasegawa et al., 2011; Yagi and Fukahata, 2011] indicate that the 2011 Tohoku-oki earthquake released nearly all the stored shear stress, our findings suggest that small earthquakes prior to the mainshock also released a large fraction of the accumulated shear stress. Note that the absolute values of the stress drops of small earthquakes are not well constrained due to assumptions such as the choice of source models, whereas the relative values among the stress drops of small earthquakes are better resolved. Therefore the hypothesis of nearly complete stress drops for the small earthquakes needs to be confirmed by other approaches.

In addition, the frequency dependence of the seismic radiation observed during the mainshock, with proportionally higher frequencies coming from the deeper parts of the fault, mimics the depth dependence we see in small earthquakes in the same region.

These results imply that smaller pre-mainshock earthquakes can provide insights into the fault properties and consequent rupture processes of future megathrust earthquakes.

Keywords: The 2011 Tohoku-oki earthquake, Stress drop, Miyagi-oki, Spatial Heterogeneity of Fault Properties

Broad-band source image for the 2011 Tohoku earthquake constructed by strong-motion data

KUBO, Hisahiko^{1*} ; ASANO, Kimiyuki¹ ; IWATA, Tomotaka¹ ; AOI, Shin²

¹DPRI, Kyoto Univ., ²NIED

From the comparison between slip model using long-period (10s \sim) seismic waves and excitation zones of short-period (0.1-10s) seismic waves, it has been suggested that the 2011 Tohoku earthquake (Mw9.1) has the period-dependent spatial variation on the seismic-wave radiation and this variation would be caused by the spatial difference of slip behavior on the plate boundary (e.g., Koper *et al.*, 2011; Lay *et al.*, 2012). However, their studies were based on the qualitative comparison of the results obtained by different methods, and the quantitative comparison between source models having different period-bands has not been made. Therefore, the construction of the source models at different period-bands by a common method is important to further understand the source characteristics of the 2011 Tohoku earthquake. Kubo et al. (2013, Fall Meeting of SSJ) estimated the spatiotemporal slip models for the 2011 Tohoku earthquake on three different period bands (10-25s, 25-50s, and 50-100s). In this study, we estimate the source models for the 2011 Tohoku earthquake on five continuously-different period bands (10-25s, 17-33s, 25-50s, 33-67s, and 50-100s) using strong-motion data, and construct broad-band source image for the 2011 Tohoku earthquake.

The spatiotemporal rupture history is estimated by the kinematic linear waveform inversion using multiple time windows (Hartzell & Heaton, 1983). The Green's functions are calculated by the 3D FDM (GMS; Aoi & Fujiwara, 1999) using a 3D velocity structure model, Japan Integrated Velocity Structure Model Version 1 (Koketsu *et al.*, 2012). Three components of velocity waveforms at 25 stations of K-NET, KiK-net, and F-net of NIED are used in this analysis. Using waveform records at the stations for the middle-size events which occurred in the source area of the 2011 Tohoku earthquake, we confirmed the adequacy 3D velocity structure model at the analyzed period-band.

The source image for the 2011 Tohoku earthquake on the period band of 10-100s is summarized as follows: (1) (1st) Deep rupture off Miyagi rupture at 0-60s toward down-dip mostly radiating relative short period (10-25s) seismic waves. (2) Shallow rupture off Miyagi at 45-90s toward up-dip with long duration radiating long period seismic wave. (3) (2nd) Deep rupture off Miyagi at 45-90s toward down-dip radiating long period (25-100s) seismic waves. The dominant-period difference in the seismic-wave radiation between twice deep ruptures off Miyagi may result from the mechanism that the second rupture is smoother than the first one because small-scale heterogeneities on the fault are removed by the first one. (4) Deep rupture off Fukushima at 90-135s.

The broad-band source model on the period band from 5-100s is under construction and we will report this.

[Acknowledgments] The strong-motion data recorded by K-NET, KiK-net, and F-net of NIED was used for this analysis.

Keywords: The 2011 Tohoku earthquake, Broad-band source image, Source models on different period bands, Source inversion, Strong-motion data

Foreshocks implying slow slip transients leading to large earthquakes

KATO, Aitaro^{1*} ; OBARA, Kazushige¹

¹ERI University of Tokyo

In the recent decades, a growing number of geophysical evidences has clarified that a major fault zone along plate interface hosts not only the unstable fast sliding during rupture of ordinary earthquake, but also slow slip transients without any seismic radiations. Because slow slip transients quasi-statically release the shear stress in the adjacent seismogenic regions, the slow slip transients may have caused stress loading on the nearby seismic patch and might play a role in a slow nucleation process leading to a large earthquake (Beroza and Ide, 2010; Bouchon et al., 2011; Kato et al., 2012). Therefore, it is quite important to reveal interplay between slow slip and unstable fast slip, in order to shed light on the nucleation process of large earthquake.

Here, we explored foreshock activities implying slow slip transients leading up to large earthquakes. We applied the matched filter technique to continuous waveform data around 10 days prior to the past large earthquakes in Japan ($M > \sim 6.5$), and created newly foreshock catalog for each sequence. We found out accelerating seismicity preceding some large earthquakes at plate interfaces and intraplate at time scales of days to hours. These foreshocks were located very close to the initiation point of each mainshock rupture. The increase in foreshock seismicity implies that a fault may begin to slowly slip before large earthquake, as like recognized in the foreshock sequence prior to the 2011 Tohoku-Oki earthquake.

Similar Characteristics between the earthquake source process and Vere-Jones' Branching model

ZHUANG, Jiancang¹ ; WANG, Dun^{2*}

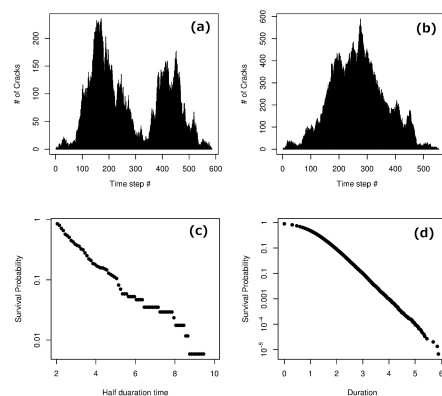
¹Institute of Statistical Mathematics, ²Earthquake Research Institute, University of Tokyo

Vere-Jones' branching crack model was developed in 1970s. In this model, the earthquake source is regarded as the results of the total population of crack elements in a critical or near-critical branching process, where the crack does not propagate in a single continuous movement, but through a series of steps. At each step, each crack element simply terminates or generates several other crack elements nearby. Regarding the total number of steps (generation) as the duration time and the total number of crack elements as the total energy released, the following similarities are found between earthquake sources and this model:

1. The distribution of energies is asymptotically a Pareto distribution (power law) for the critical case, or a tapered Pareto distribution (tapered power law, Kagan distribution) for the subcritical case.
2. The duration time of ruptures has a tapered inverse power distribution.
3. The number of crack elements at each generation (time step) show similar patterns of earthquake source time functions.

Figure 1 (a) and (b): Plots of the numbers of crack elements at each time step in two simulation examples. (c): Distribution of half duration times in real earthquake catalog. (d): Distribution of duration times in synthetic catalogs.

Keywords: Branching process, Gutenberg-Richter Magnitude-Frequency Relation, Tapered Pareto distribution, Earthquake source



Review on Source Type Diagrams

ASO, Naofumi^{1*} ; OHTA, Kazuaki¹ ; IDE, Satoshi¹

¹Graduate School of Science, The University of Tokyo

Force system of earthquake is expressed by a symmetric moment tensor, assuming internal forces on a point source, and it has information of characteristic directions, source size, and source type. Although we often assume double couple as the source type, significant non-double-couple component including isotropic component is reported mainly for induced earthquakes or volcanic earthquakes. It is also known that combination of double couples may produce non-double-couple components. For discussion on source types, it is helpful to display them into some visual diagrams.

Since the information of source type has two degrees of freedom, it can be displayed on a two-dimensional flat plane. Although the diagram developed by Hudson et al. [1989] (HPR diagram) is popular, it is inconsistent with the concept of scalar moment [Aki and Richards, 2002]. This problem originates in the projection of a three-dimensional point ($\lambda_1, \lambda_2, \lambda_3$) on a cubic surface, where λ_1, λ_2 , and λ_3 are eigenvalues of moment tensor.

Then, Chapman and Leaney [2012] developed a new diagram by combining spherical projection and stereographic projection (CL diagram). The spherical projection overcomes the problem of the HPR diagram, and the stereographic projection keeps areal density from a spherical surface to a flat plane. This diagram has an advantage that a straight line passing through the center corresponds to the mechanism obtained by combination of an arbitrary mechanism and a double couple, but the diagram is curved shape, and it does not suit for detailed discussions on non-double-couple component when the isotropic component is dominant.

In the present study, we developed another new rectangle diagram that overcomes difficulties of the HPR diagram and the CL diagram simultaneously (AOI diagram). After projecting ($\lambda_1, \lambda_2, \lambda_3$) on a spherical surface, we project it on a cylinder, keeping areal density. This diagram is an orthogonal system of the isotropic axis (the trajectory for varying isotropic component) and the deviatoric axis (the trajectory for varying deviatoric component while keeping its scalar moment). Since isotropic component represents the information from P-wave and deviatoric component represents the information from both P- and S-waves equivalently, the AOI diagram is consistent with the concept of seismogram analyses.

Since there is no source type diagram that is the best at everything, as well as map projection, it is important to use various diagrams taking account of their advantages and disadvantages. In the present study, we also provide examples of projecting a data set on different diagrams, and point out their apparent differences and important considerations.

Keywords: moment tensor, source type diagram, double couple, CLVD, isotropic deformation

Stress concentration ahead of supershear rupture

FUKUYAMA, Eiichi^{1*} ; XU, Shiqing¹ ; MIZOGUCHI, Kazuo² ; YAMASHITA, Futoshi¹

¹Nat'l Res. Inst. Earth Sci. Disas. Prev., ²Centr. Res. Inst. Elect. Pow. Ind.

We report the shear strain field ahead of a supershear rupture. The strain data was obtained during the large-scale biaxial friction experiments conducted at NIED in March 2013. We conducted friction experiments using a pair of meter-scale gabbro rock specimens whose fault area was 1.5m x 0.1m. We applied 2.6MPa normal stress and loading velocity of 0.1mm/s. At the long side of the fault edge, which is parallel to the slip direction, 32 2-component semi-conductor strain gauges were installed at an interval of 50mm and 10mm off the fault. The data are conditioned by high frequency strain amplifiers (<0.5MHz) and continuously recorded at an interval of 1MHz with 16-bit resolution. Many stick slip events were observed and a unilateral rupture event was chosen in this analysis that propagated with supershear rupture velocity. By focusing at the rupture front, stress concentration was observed and sharp stress drop occurred immediately inside the rupture. We found that the stress concentration becomes mild as the rupture propagates and length of the stress concentration area becomes longer. This observation is quite interesting because the rupture propagates at a constant speed close to square root two times the shear wave velocity and thus a longer stress concentration region suggests more energy dissipation. We might speculate that such longer stress concentration area suggests longer plastic region ahead of the rupture (or longer cohesive distance). I.e. The cohesive zone length might be longer as the rupture propagates to maintain constant rupture velocity propagation.

Keywords: Earthquake rupture, Stress concentration, Supershear rupture

Effects of normal stress on the evolution of AE activities and frictional properties of a fault

IIDA, Takuro¹ ; YABE, Yasuo^{1*}

¹Graduate School of Science, Tohoku University

To numerically investigate earthquake generations on a plate interface or a fault, we need to know their frictional properties. This study provides a clue to evaluate the frictional properties from spatio-temporal variations of such observations as seismicity and aseismic sliding on the interface of the fault.

We performed frictional sliding experiments using a rotary shear apparatus under a variety of normal stress from about 5 MPa to about 15 MPa. Stepwise change in the sliding rate was imposed to investigate rate dependences of AE activity and friction. Cumulative displacement up to 200 mm was achieved to elucidate their evolutions.

We confirmed similar evolutions of AE activities and friction to those shown by Yabe (2002). That is, the frictional property (rate dependence of friction) of the fault was first the velocity strengthening. The velocity strengthening became weak with an increase in the cumulative sliding. Then, the fault showed the frictional property of velocity weakening. Finally, the rate dependence of friction converged to a constant negative value, when the cumulative sliding reached a critical distance. The m -value of AE events increased with sliding, when the cumulative sliding distance was smaller than a critical distance. After the critical sliding distance, the m -value took a constant value. The critical sliding distances of the frictional property and the m -value were almost the same each other. The rate dependence of the m -value, which was negative under a small sliding distance, also converged to a constant value of about zero at the cumulative sliding distance.

The evolutions were quantitatively evaluated by applying an exponential-decay function to data that is similar to the function proposed by Wang and Scholz (1994) to express wear processes of a fault. The function well reproduced the experimental data, suggesting that AE activities and frictional properties evolved in association with the wear. The decay distances of evolutions of the AE activities and the frictional properties were equal to each other and in inverse proportion to the normal stress. The latter could be understood by taking into account that the larger the overlap volume of asperities on the fault, the larger the normal stress. Further, when the normal stress was increased, the velocity weakening became weak and the m -value was decreased.

These results imply that there exists interrelations among seismicity and frictional properties of the fault.

Keywords: frictional sliding, AE activity, frictional property, rotary shear, evolution, normal stress dependence